ANOMALOUS FATIGUE BEHAVIOR IN POLYISOPRENE*

C. M. ROLAND

NAVAL RESEARCH LABORATORY, CHEMISTRY DIVISION, CODE 6120, WASHINGTON, D.C. 20375-5000

AND

J. W. SOBIESKI

GEO-CENTERS, INC., FORT WASHINGTON, MARYLAND 20744

INTRODUCTION

Material failure corresponds to the propagation of damage to a catastrophic level. Fracture is made possible when the strain energy release rate (*i.e.*, the tearing energy) exceeds a critical value. This tearing energy is defined as[1-3]

$$T = -t^{-1}(dU/dc), \tag{1}$$

where t is the specimen thickness, U the stored energy, and c the crack length. The value of T associated with catastrophic failure is a material property referred to as the fracture energy or tear strength. The tensile strength or breaking stress of the material is the stress at which the strain energy release rate attains this critical value. Below the level of tearing energy necessary for catastrophic failure, mechanical crack propagation proceeds at a finite rate (*e.g.*, per number of cycles, N) that can often be described by a power law relation,

$$dc/dN = aT(c)^b, \tag{2}$$

where a and b are presumed material constants. When the tearing energy is insufficient for mechanical crack growth, in unsaturated rubbers, chemically induced chain scission (*e.g.*, by reaction with ozone) transpires at a rate that is essentially independent of the tearing energy.

For a tensile deformation, Equation (1) takes the form

$$T = 2kUc/V, \tag{3}$$

where V is the volume of deformed material and k a geometric factor that depends weakly on the elongation, e[3]

$$k = (1 + e)^{-1/2}. \tag{4}$$

The magnitude of the strain energy release rate for tensile straining thus increases in proportion to the extent of crack growth, so that the rate of crack propagation accelerates rapidly ($b > 2$). The fatigue lifetime, N_f, or number of

---

* Based on a paper presented at a meeting of the Rubber Division, American Chemical Society, Cincinnati, Ohio, October 18-21, 1988. B.

deformation cycles required for the inherent flaw size, c_0, to grow to the critical magnitude, c_c, for catastrophic failure, is[3,4]

$$N_f = a^{-1} \int_{c_0}^{c_c} T(c)^{-b} dc. \tag{5}$$

For tensile deformation,

$$N_f = (a - ab)^{-1}(2kU/V)^{-b} c_0^{1-b}, \tag{6}$$

since $c_c \gg c_0$.

This report is concerned with the effect on the fatigue life and other failure properties of rubber of imposition of a period of annealing in a strained state.

EXPERIMENTAL

The *cis*-1,4-polyisoprene was either *Hevea Brasiliensis*, NR (SMR-L from the Ore and Chemical Corporation) or the synthetic variant, IR (Natsyn 2210 from The Goodyear Tire and Rubber Co.), and the styrene–butadiene copolymer was solution-SBR with 22.5% styrene (Duradene 706 from the Firestone Tire and Rubber Company). Stock formulations are given in Table I. Curing was done at 160°C for 30 min.

Using an Instron 4206, uniaxial deformation data was obtained both at 0.1 sec^{-1} and in equilibrium. For the latter, the test specimen was elongated to the desired strain and the force measured continuously until cessation of the stress relaxation. Stress relaxation behavior was characterized using an Imass Corp. Dynastat Mark II instrument. Tensile fatigue testing was conducted along the lines of ASTM D 4482-85 using a Monsanto Fatigue To Failure Tester. In this procedure, the specimens are cycled a few hundred times, after which the set that developed is removed by displacement of the test fixture crosshead. The minimum of the dynamic fatigue deformation thus corresponds to zero stress. In order to avoid errors due to switch bounce, the counters in the Tester were replaced with a parallel interface board connected to a microcomputer. The maximum amplitude of the dynamic deformation was typically 124% elongation. As described below, in some cases the testing was interrupted after a number of cycles and the specimens annealed under different conditions for various durations. A minimum of eight specimens were used per test. Cut-growth mea-

TABLE I

RUBBER COMPOSITIONS

Designation	NR-1	NR-2	IR-1	SBR-1
NR	100	100	—	—
IR	—	—	100	—
SBR	—	—	—	100
N-326	—	60	—	—
Antioxidant	0.5	0.5	0.5	—
Dicumyl peroxide	1.0	1.2	1.0	0.1

surements were obtained from initially precut specimens deformed in tension using an MTS apparatus.

RESULTS

In Table II are displayed fatigue lifetimes for an IR-based stock measured according to the ASTM D 4482-85 procedure. In some cases the fatigue deformation was halted after a number of cycles and the test specimens maintained at either the maximum or minimum dynamic strain amplitude for a time period, followed by resumption of the fatigue testing. Such interruption of the cycling markedly altered the fatigue results (Table II). Crack propagation, although usually associated with cyclical deformation, is nevertheless known to transpire when an elastomer is maintained in a constant (no cycling) strained state. While it might therefore be expected that reduction in the number of deformation cycles required for failure would accompany the imposition of a period of constant strain in the course of the usual fatigue experiment, the behavior illustrated in Table II is more complicated. Annealing at elevated strain (*e.g.*, 124% elongation) increased the fatigue lifetime relative to the results for uninterrupted fatigue testing. Such improvement was typically observed after 24 h or more

TABLE II

EFFECT OF ANNEALING ON FATIGUE BEHAVIOR OF IR-1 (DYNAMIC STRAIN = 124%)

Prekilocycles[a]	Annealing strain	Annealing time, min	Fatigue lifetime, kilocycles
—	—	—	156
0.2	12	1440	90
0.2	124	1440	206
0.2	12	2880	46
0.2	124	2880	170
40	—	—	154
40	12	1440	142
40	124	1440	170
40	12	4320	77
40	124	4320	203
40	12	4320[b]	82[b]
40	124	4320[b]	267[b]
40	12	4320[c]	64[c]
40	124	4320[c]	147[c]
40	0	4320[d]	189[d]
40	12	4320[d]	184[d]

[a] Number of fatigue kilocycles prior to annealing.

[b] After annealing specimens heated to 110°C in strained state immediately prior to resumption of fatigue cycling.

[c] After annealing specimens heated to 110°C in unstrained state immediately prior to resumption of fatigue cycling.

[d] Annealing executed in vacuum at room temperature.

TABLE III

EFFECT OF ANNEALING ON FATIGUE BEHAVIOR OF NATURAL-RUBBER-BASED STOCKS[a]

Stock	Annealing strain	Annealing time, min	Fatigue lifetime, kilocycles
NR-1	12	4320	56
NR-1	124	4320	179
NR-2	—	0	54
NR-2	12	4320	45
NR-2	124	4320	55

[a] Prekilocycles = 0.2, dynamic strain = 124%.

annealing at 124% extension. On the other hand, when the annealing was executed at the minimum of the strain cycle (corresponding to zero dynamic stress) there was a dramatic decrease in the total number of fatigue cycles required for failure. Results similar to these were also obtained with NR-based stocks and with filled compounds (Table III). The improvements in fatigue life accompanying annealing at high strain, as well as the reduction in lifetime due to annealing at the minimum dynamic strain amplitude, were significant and reproducible, notwithstanding the large scatter inherent in failure property measurements (see Figure 1).

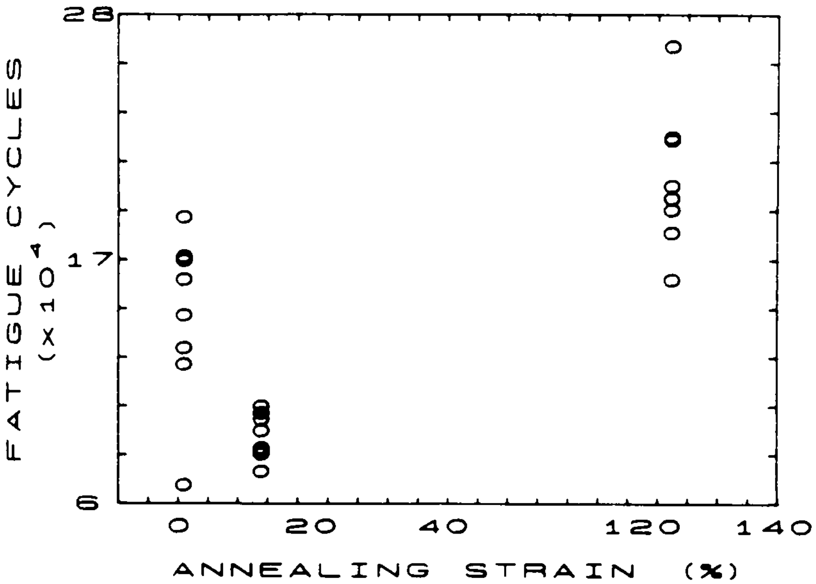

FIG. 1. The influence of annealing for 24 h at various strains on the fatigue lifetime of IR 1. The results for each individual test specimen are shown in order to demonstrate that the decrease at low annealing strain, as well as the improvement at higher annealing strain, exceed the experimental scatter in the measurements.

TABLE IV

EFFECT OF ANNEALING ON EQUILIBRIUM SWELLING (IN CYCLOHEXANE) AND OPTICAL DENSITY

Sample	Swelling ratio	Transmission (at 500 nm)
NR-1 unannealed	0.16	12%
NR-1 annealed 72 h at 124% strain	0.16	1%
SBR-1 unannealed	0.17	15%
SBR-1 annealed 72 h at 124% strain	0.16	3%

This annealing does not measurably alter the crosslink density (Table IV), suggesting that the influence of annealing on fatigue life is not a bulk phenomenon. Some alteration is taking place during annealing either of the cracks present in the specimens or of the rubber immediately adjacent to the cracks. Fatigue and tensile strength reflect identical phenomena—the growth of flaws and concurrent (at least for uniaxial extension) increase in tearing energy up to the point of failure. Accordingly, the effect annealing has on tensile strength can be compared to its effect on fatigue life. Displayed in Figure 2 is the tensile strength measured for NR-1 annealed 72 h at various strains. Two characteristic features are in evidence. At low annealing elongations (*ca.* 10%), a minimum in tensile strength is attained. As the strain during annealing is increased, there

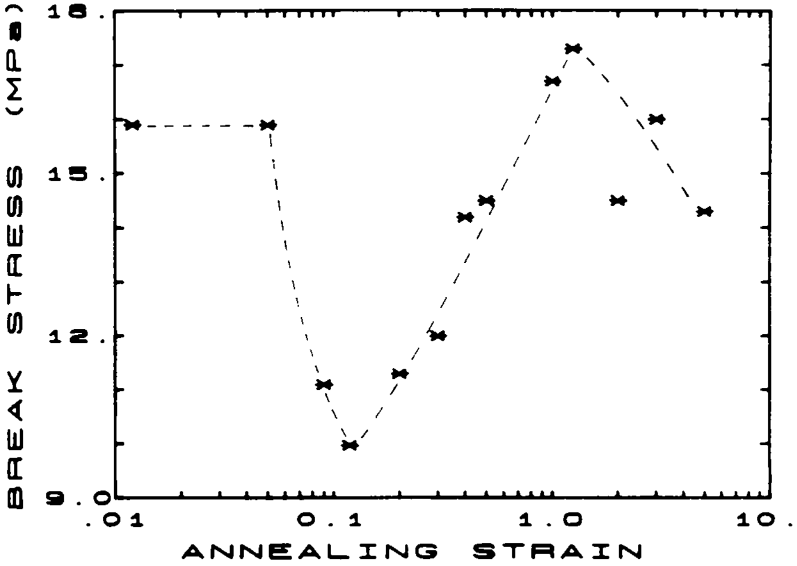

FIG. 2.—The tensile strength of NR-1 after annealing for 72 h at the indicated elongation. The results, each representing the average of eight measurements, had an average deviation of about 1 MPa.

is a corresponding increase in the subsequently measured breaking stress. At sufficiently high annealing strains, the measured strength exceeds the original (unannealed) tensile strength. The general similarity between Figure 2 and the data in Table II suggest similar mechanisms are operative in both the fatigue and the tensile strength experiments.

FATIGUE LIFE REDUCTION

In contrasting the fatigue and strength results, it is noted that during fatigue cycling, the adjustment to remove buckling of the test specimens due to unrecovered strain (the set) was equivalent to 12% elongation. Although exact correspondence would be coincidental, it is instructive that the minimum in Figure 2 occurs roughly at the dynamic strain during cyclical fatigue associated with zero stress. The annealing during the fatigue experiments was conducted at this minimum dynamic strain. The stress, however, does not remain zero when the fatigue cycling ceases. The stress increases over time, eventually leveling off at the equilibrium value associated with that strain. To illustrate this, in Figure 3 are shown stress relaxation measurements for the NR-1 after imposition of a large step strain, which is then reduced to a smaller tensile strain. On return of the specimen to the lower strain, a stress undershoot is observed (congruent with a permanent set), after which the equilibrium stress is attained in a time period which depends on the duration of the initial (larger) strain. The set in the material is not permanent, and recovers over the same time scale. The transitory zero stress at a nonzero strain is due to inhomogeneous deformation on

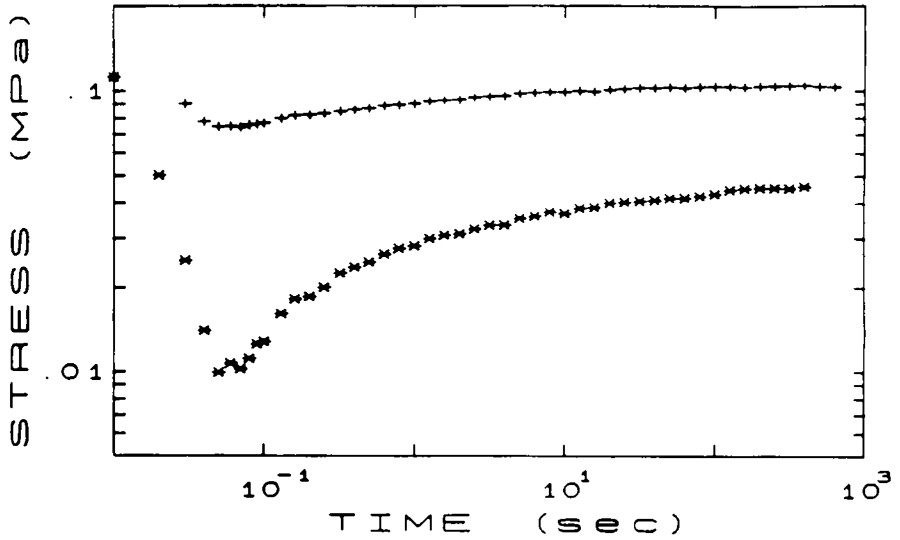

FIG. 3.—Stress relaxation in NR-1 during a reversing double step strain. The initial extension was 135% for 2 min followed by a 10% strain (+++) and for 120 min followed by a 5% strain (***). Zero on the abscissa corresponds to the time at which the second step was imposed.

the molecular level, with network strands present in both extended and compressed configurations[5]. Thus, when imposed during the course of a fatigue experiment, annealing at a strain corresponding to zero dynamic stress becomes annealing at a stress level that increases to some constant value over time.

The effect of low-strain annealing on fatigue behavior is essentially equivalent to the effect on tensile strength. In both cases, small, but non-negligible static stresses give rise to a deterioration in performance. The observation of losses in tensile strength and fatigue lifetime after annealing at very low strains is also found in both IR- and SBR-based rubbers (with representative results seen in Figures 4 and 5).

Surface cracking.—At annealing strains greater than those associated with the minimum in failure properties, samples exhibit a readily apparent whitening (Table IV). Scanning electron micrographs reveal this whitening to be due to extensive cracking at the surface of the specimens (Figure 6). Contrarily, when annealing at low strains (*ca.* 10%), even after several days, no whitening of the samples arises, although a few surface cracks become visible. At higher annealing strains, such large cracks never appear. As annealing at higher strains (>20%) is continued, the region of the material with an abundance of small (on the order of a μm) surface cracks extends progressively deeper into the rubber. The severity of the surface damage also increases over the first couple of days.

When the annealing of test specimens is executed in vacuum (Table II), there is no large reduction in fatigue life or strength of the rubber, nor is any surface cracking observed. From this and the observation that the cracking in air is confined to the surface, it is clear that the damage accumulating during the course of annealing is due to chemical attack, specifically, reaction with ozone.

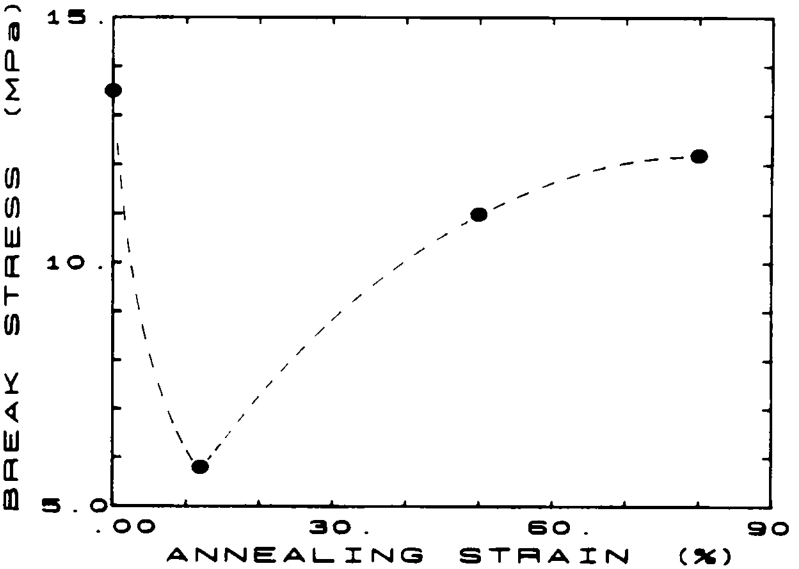

FIG. 4.—The tensile strength of IR-1 after annealing for 72 h at the indicated strain.

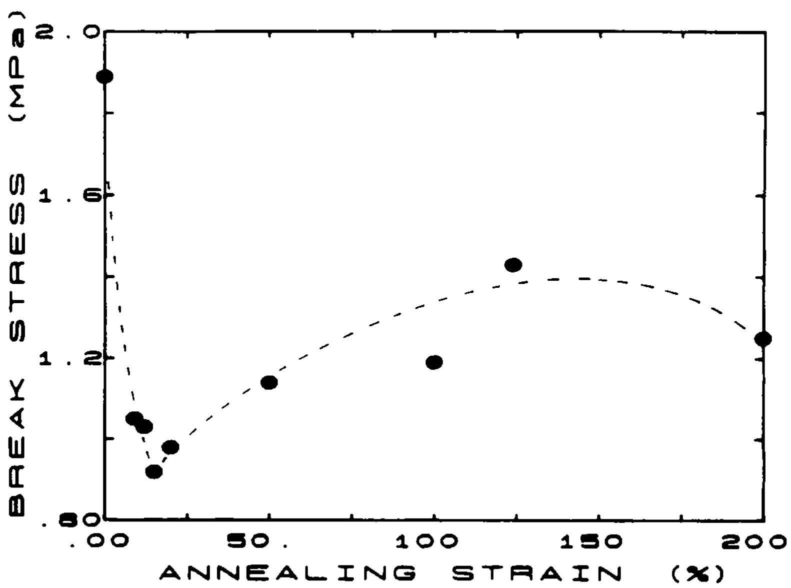

Fig. 5.—The effect of annealing (for 72 h) of SBR-1 at the indicated tensile strains on the subsequently measured stress at break. Although the data for duplicate testing were not normally distributed, a standard deviation of 0.05 MPa was calculated.

It is known that ozone readily reacts with unsaturated hydrocarbons[6,7]. When the strain is low, the strain energy release rate, which for uniaxial extension is proportional to the product of crack length and strain [Equation (3)], is sufficient to effect ozone cracking only for the largest flaws present. These larger flaws thus grow in size with the concomitant reduction in the rubber's fatigue life or strength as seen in Tables II and III and Figures 2, 4, and 5. At higher annealing strains, the strain energy is high enough that many of the cracks initially present experience the level of tearing energy necessary for stress-induced ozone cracking. An abundance of microcracks thus develops, with this high concentration causing mutual interferences. The stress is not amplified at the tip of these surface flaws because neighboring cracks have released the strain energy of the material at the crack tips. Accordingly, at higher annealing strains, cracks do not experience the continual growth occurring at lower strains. Consequently, annealing at low strains is more deleterious than that done at high strains because only the largest flaws determine the failure properties [see Equations (3) and (6)]. Note that the extensive damage originating at the surface when the annealing is done at higher strains does not *per se* reduce the strength since this damage region represents only a small fraction (1 or 2%) of the total material. Strain amplitude effects such as these on the nature of ozone cracking have been previously described by various investigators[8-11]. The influence of annealing at the minimum dynamic strain during the course of a fatigue experiment is an equivalent phenomenon upon recognition that the zero stress associated with this strain becomes nonzero upon cessation of the cycling.

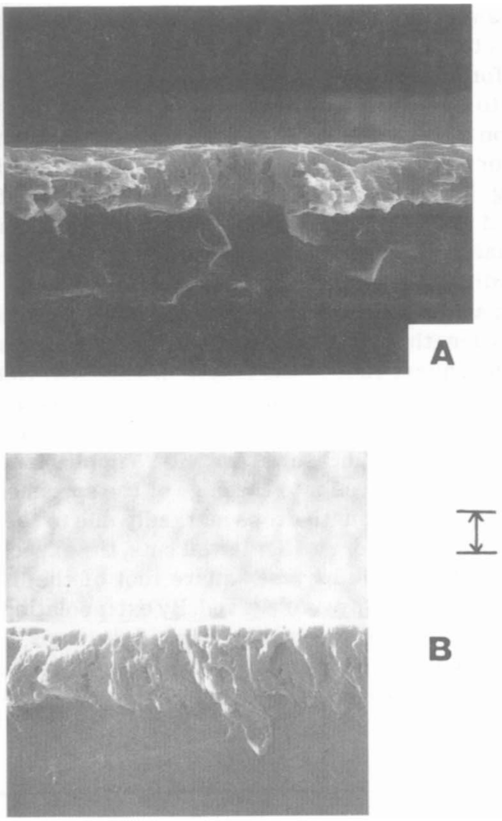

FIG. 6.—Scanning electron micrographs of the surface damage accumulating in NR-1 after (A) 72 and (B) 288 h of annealing in air at 124% elongation (the scale mark indicates 20 μm). As can be seen in these edge views, the region of pervasive microcracking extends about 30 μm into the bulk of the material.

In principle, the time required for build up of the stress after the cycling ceases could be calculated. The time required for cessation of measurable stress relaxation in this material is on the order of 100 s. In the range of linear viscoelastic behavior, it is then expected that when a sample is maintained after cessation of cycling at the strain corresponding to zero dynamic stress, the stress will build up to the static equilibrium value in roughly this 100 s. In the presence of reversing strain cycles, however, crosslinked rubber diverges from linear viscoelastic behavior at strains well within the domain of linearity as judged by the usual methods (*e.g.*, strain independence and time invariance of the mechanical response)[5]. The induction time for any stress-induced ozone cracking, therefore, can only be accurately determined by direct measurement.

Crack size characterization.—It is useful to make more quantitative the explanation for the loss of properties when a fatigue experiment is interrupted. For example, it is interesting to note that the fraction of the fatigue life transpiring prior to annealing has a significant influence on the ultimate behavior. Figure 7 displays the tensile strength measured immediately after annealing at various strains for 72 h in air. The various curves represent different extents of cycling prior to imposition of the annealing. A minimum in the dependence of the strength on annealing strain is observed when as many as 40 kilocycles are executed prior to annealing. If a greater fraction of the lifetime has expired before annealing, however, annealing has no measurable effect on the subsequently measured tensile strength. To account for these results, it is necessary to consider the nature and growth of the flaws initially present in the material. When the tip radius of the crack is much smaller than its length, the stress intensification in an elastic material will be directly proportional to the square root of the crack length^{3,12}. This means that the breaking stress should vary inversely with the square root of the length of the flaw. Notwithstanding significant deviations from elastic mechanical behavior, this relationship between flaw size and tensile strength has previously been verified for rubber^{3}. Figure 8 shows the tensile strength measured for NR-1 samples in which razor cuts of various length were introduced into the edge of the specimens. For sufficiently large precuts, the tensile strength drops markedly due to the absence of strain-induced crystallization^{13,14}. For smaller initial cuts, the expected proportionality of the tensile strength to the inverse square root of the flaw size (the latter measured by optical microscopy) is observed. By extrapolating this linear portion of the curve to the measured strength of uncut specimens, a value of 70 μm is deduced for the maximum inherent flaw size. From the measured dependence of the crack-growth propagation rate (expressed as meters per cycle) on tearing energy (in MJ per square meter),

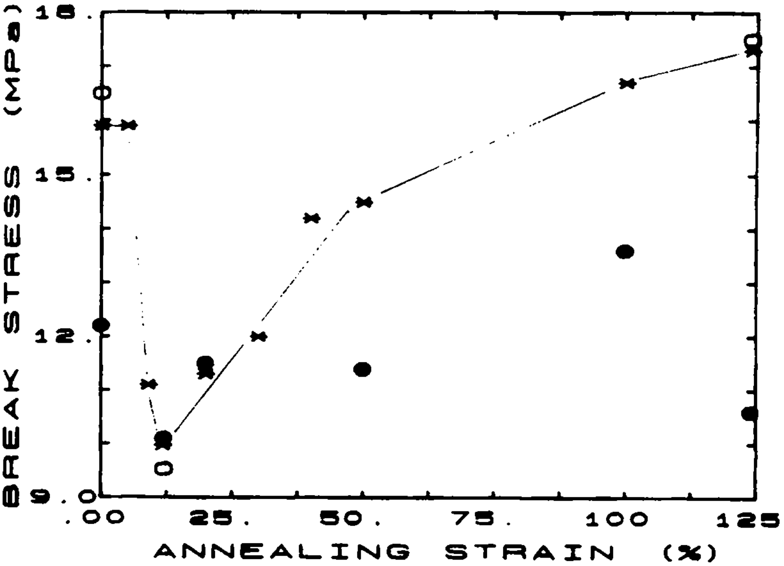

FIG. 7.—The effect on the tensile strength of annealing NR-1 at various strains. The 72 h annealing period commenced after (*) 200, (O) 40 000, and (●) 80 000 fatigue cycles at 124% elongation.

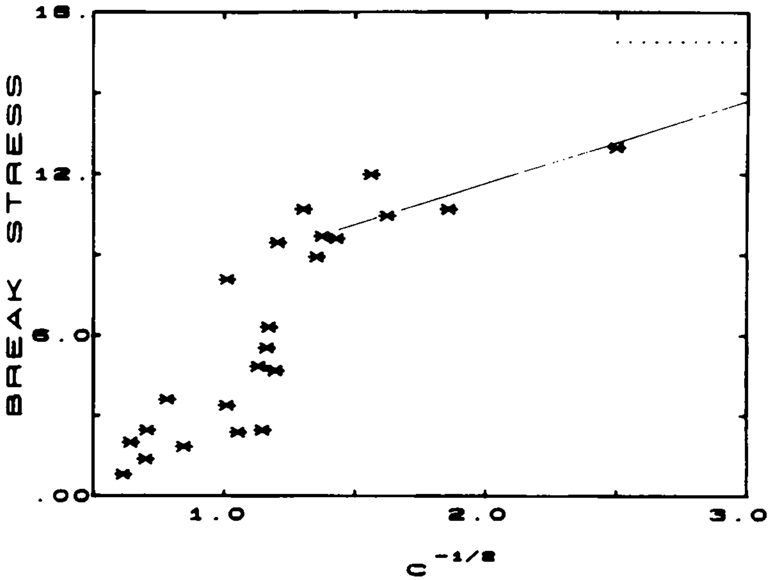

FIG. 8.—The relationship between the tensile strength of NR-1 and the length of an edge precrack. From the tensile strength measured for samples without intentionally introduced cuts (designated by the horizontal dotted line), the inherent flaw size is estimated to be about 70 μm.

$$dc/dN = 2 \times 10^{-7} T^3, \tag{7}$$

the length of the largest flaw after a given duration of fatigue cycling can be estimated. Using Equations (5) and (7), this crack length is found to vary according to

$$c(N) = (4.2 \times 10^{16} - N/2.1 \times 10^{-12})^{1/4}. \tag{8}$$

Applying Equation (8), it is seen that the first 40 fatigue kilocycles only increase the length of a 70 μm crack by about 15%. Any crack growth occurring during annealing imposed through the first 40 kilocycles will consequently have a very significant effect. The crack size roughly doubles over the next 40 kilocycles, however, with the original flaws now on the verge of becoming visible to the naked eye. At this point, the residual fatigue lifetime is very small. Small increments in flaw size that may be effected by ozone cracking during annealing now will have a negligible effect on the ultimate properties. The results seen in Figure 7 are thus consistent with the flaw sizes and their change with fatigue cycling.

FATIGUE LIFE IMPROVEMENT

The loss of failure properties at low annealing strains is seen to result from ozone-induced growth of inherent flaws. At higher strains (>20%) the high concentration of microcracks causes relaxation of stress at the surface of the material so that there is less effective elevation of the stress at the flaw tips. The loss of performance at low annealing strains and the absence of such a loss at higher annealing strains can thus be satisfactorily explained. However, after annealing at very high strains (>100%), the fatigue life and tensile strength of the NR and IR stocks attain a level exceeding that of the initial, unfatigued, samples (see, for example, Table II and Figures 1 and 2). Since the bulk properties are not affected by the annealing (Table IV), these improvements in failure properties must be attributable to either a change in the stress concentration about an existing flaw or to a change in the material in proximity to the flaw. Specific potential mechanisms for the improvements in performance are now examined.

Hypoelasticity.—It is conceivable that during annealing at high strain, sufficient additional relaxation of stress may transpire, whereby the crack growth immediately upon subsequent fatigue cycling would be slower due to a reduced strain energy density. Although relaxation occurs during cycling, annealing may enable a greater extent of stress dissipation. The term hypoelasticity refers to such a process. Not inconsistent with this idea, when the time of annealing was shortened to only a few minutes, no significant improvement in fatigue life resulted. By heating the sample during the annealing, any relaxation should be accelerated, so that a brief (high temperature) annealing might be sufficient to effect an increase in the subsequent fatigue life. In fact, however, heating in the strained state did not lead to better failure properties if the annealing period was short.

The annealing experiments were modified such that fatigue life and strength measurements were made, not immediately after annealing, but rather 24 h later (with the specimens maintained in an unstrained condition in the interim). Any relaxation during annealing in the strained state would be lost as the samples were kept unstrained for the 24 h. Nevertheless, the fatigue lives and tensile strengths were found to exhibit the same increase over unannealed samples as when the specimens were tested immediately after annealing. This argues conclusively against any significant contribution to the ultimate properties from relaxation during annealing.

Finally, it is noted that an SBR sample, which presumably would also benefit from hypoelastic effects since its relaxation times were measured to be of the same order of magnitude as that of the polyisoprene stocks, did not exhibit the improved failure properties seen in the NR and IR materials (Figure 5).

Damage accumulation.—Since any changes (*i.e.*, increases) in crack length during annealing could only reduce the subsequent performance of the rubber, improvements after high-strain annealing are unrelated to crack size *per se*. It is known, however, that the region of material adjacent to a crack is usually replete with damage[15,16]. The nature and extent of this damage, moreover, are sensitive to any deformation experienced by the material[15,16]. In view of this, it is likely that the volume of rubber in proximity to major cracks will be altered by annealing at high strains. The interesting question is whether such damage accumulation will cause a loss of performance by virtue of a weakened crack-tip region, or an improvement in properties. The latter could result from crack-tip blunting or perhaps from production of a more hysteretic, and thus tougher, material in the path of the advancing crack. Although the existence in rubber of an evolving defect region near cracks has been established[15], assessment of its contribution to material performance warrants further study. Accordingly, the relevance of local damage accumulation to the results obtained in the present study is unknown.

Orientational crystallization.—When either of the unfilled polyisoprene-based rubbers was stretched up through about 500% elongation, the measured elastic (equilibrium) stress was found to be in accord with the Mooney-Rivlin description of the strain dependence of this stress[5]. Beyond this extension, the equilibrium stresses were significantly less than the values extrapolated from the lower strain results. This behavior indicates the existence of strain-induced crystallization in these rubbers at high strains. A tensile elongation of 500% was also found to be the minimum necessary for observation of the x-ray diffraction pattern associated with oriented crystallinity. The high-strain annealing during the course of fatigue cycling was conducted at a strain of 124%, which is well below the level necessary for strain crystallization at these crosslink densities. This absence of bulk crystallinity at an annealing strain of 124%, however, does not preclude local crystallization at the tip of a crack. For an elastic material, the strain amplification is equal to twice the square root of the ratio of the crack length to crack radius[12]. The amplification in the vicinity of the tip of a 70 μm crack would easily be sufficient to effect localized strains in excess of 500% for a bulk strain of 124%. This means that strain-induced crystallization is transpiring at least at the crack tip in annealed specimens. Such crystallization will effect superior fatigue and strength performance, and thus likely underlies the improvements in the NR and IR compounds after annealing at high strain.

Of course, the rubber experiences this same high strain during the fatigue cycling itself; however, crystallization is not completed during the brief residence time at the peak strains during cycling. This fact can be gleaned from Figure 9, in which the relaxation time measured for the NR-1 is displayed *versus* strain. At strains sufficient for orientational crystallation, there is a large increase in the apparent relaxation time. This increase is due to a process other than simple viscoelastic relaxation; it reflects the time scale of the crystallization. This crystallization can be seen to continue well beyond the time scale of a dynamic fatigue cycle. As a result, annealing at high strain allows more extensive crystallization in the crack tip region, enabling a level of material performance not obtained in the absence of the annealing.

More evidence that strain crystallization is the primary mechanism for the property improvements is obtained when, after annealing, the sample is heated for a few minutes to at least 100°C. If the heating is done in the unstrained state, the fatigue life (Table II) or tensile strength (Table V) is observed to return to the level measured for unannealed specimens. This temperature is evidently sufficient to melt the crystallites at the crack tip, at least when the sample is unstrained. If the strain is maintained during the heating, however, the reference state with regard to the thermodynamic stability of the crystallites is a highly oriented amorphous state. Under these conditions, it is expected that the crystal phase will exhibit greater stability (in the present case apparently possessing a melting point higher than 100°C) and thus remain after heating to confer higher properties.

Finally, as noted above, when a noncrystallizing rubber (SBR-1) was subjected to the high annealing strains, no increase in strength over the unannealed rubber

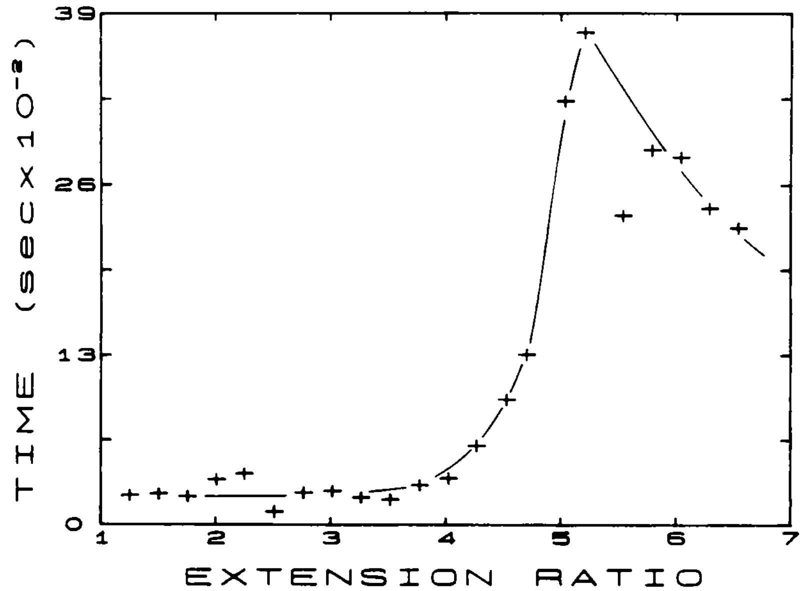

FIG. 9.—The time period required for cessation of stress relaxation in NR-1 as a function of the uniaxial extension ratio. The increases at the higher strains, which coincide with deviations in the strain dependence of the elastic modulus from the Mooney-Rivlin theory, are associated with the onset of orientational crystallization.

was realized (Figure 5). The increase in properties of the polyisoprene rubbers after the high annealing strains can be attributed to the occurrence of strain-induced crystallization.

SUMMARY

Annealing of a polyisoprene-based elastomer can result in significant changes in its failure properties, the nature of which depends on the deformation of the rubber during the annealing. Although a deterioration of properties from low-

TABLE V

EFFECT OF ANNEALING ON TENSILE STRENGTH OF NR-1

Annealed[a]	Heated	Tensile strength, MPa
No	—	15.9
Yes	—	17.3
Yes	Strained	18.0
Yes	Unstrained	16.0

[a] 72 h at 124% elongation.

strain annealing and improved performance from high-strain annealing may be contrary to intuition, the mechanisms which underlie these annealing effects are well known. The behavior described herein simply represents other manifestations of these phenomena. These alterations in performance, moreover, are readily induced at strains within the range of conventional fatigue and crack-growth experimentation, and thus demonstrate some of the difficulties in relating laboratory characterizations to the performance of materials in other environments.

ACKNOWLEDGMENTS

The authors express their appreciation to Mr. J. P. Armistead, of NRL, for assistance with the microscopy work, and to Mr. E. Greenawald, of Geo-Centers Inc., who implemented the modification of the Fatigue Tester. This work was supported in part under Office of Naval Research Contract No. n0001488WX24207.

REFERENCES

[1] R. S. Rivlin and A. G. Thomas, *J. Polym. Sci.* **10,** 291 (1953).
[2] G. J. Lake and A. G. Thomas, *Proc. R. Soc. London* **300,** 108 (1967).
[3] A. N. Gent in "Science and Technology of Rubber," F. R. Eirich, Ed., Academic Press, New York, 1978, ch. 10.
[4] G. J. Lake, RUBBER CHEM. TECHNOL. **45,** 309 (1972).
[5] C. M. Roland, RUBBER CHEM. TECHNOL. **62,** 863, 880 (1989).
[6] J. I. Cunneen, RUBBER CHEM. TECHNOL. **41,** 182 (1968).
[7] A. A. Popov and G. E. Zaikov, *J. Macromol. Sci., Rev. Macromol. Chem. Phys.* **C23,** 1 (1983).
[8] J. R. Beatty, RUBBER CHEM. TECHNOL. **37,** 1341 (1964).
[9] M. Braden and A. N. Gent, *J. Appl. Polym. Sci.* **3,** 90 (1960).
[10] M. Braden and A. N. Gent, *J. Appl. Polym. Sci.* **3,** 100 (1960).
[11] G. J. Lake and P. B. Lindley, *J. Appl. Polym. Sci.* **9,** 2031 (1965).
[12] K. Hellan, "Introduction to Fracture Mechanics," McGraw Hill, New York, 1984.
[13] A. G. Thomas and J. M. Whittle, RUBBER CHEM. TECHNOL. **43,** 222 (1970).
[14] C. L. M. Bell, D. Stinson, and A. G. Thomas, RUBBER CHEM. TECHNOL. **55,** 66 (1982).
[15] C. M. Roland and C. R. Smith, RUBBER CHEM. TECHNOL. **58,** 806 (1985).
[16] V. S. Kuksenko and V. P. Tamuzs, "Fracture Micromechanics of Polymer Materials," Martinus Nijhoff, The Hague, 1981.